Available online at www.sciencedirect.com
ScienceDirect
Journal of Power Sources 179 (2008) 837–847
JOURNAL OF POWER SOURCES
www.elsevier.com/locate/jpowsour

Study of the electro-oxidation of CoO and $Co(OH)_2$ at 90 °C in alkaline medium

Frédéric Tronel [a,b], Liliane Guerlou-Demourgues [a,*], Lionel Goubault [b], Patrick Bernard [b], Claude Delmas [a]

[a] *ICMCB-CNRS, University Bordeaux I, Site ENSCPB, 87 Avenue Dr. A. Schweitzer, 33608 Pessac Cedex, France*
[b] *SAFT - Direction de la Recherche, 111-113 Boulevard Alfred Daney, 33074 Bordeaux Cedex, France*

Received 19 September 2007; received in revised form 13 December 2007; accepted 3 January 2008
Available online 11 January 2008

Abstract

Cobalt is usually post-added as CoO or $Co(OH)_2$ to nickel hydroxide at the positive electrode (nickel oxide electrode) of alkaline batteries, to form a conductive network. In the present work, we focus on the transformation of CoO and $Co(OH)_2$ phases when oxidized at 90 °C. The Co_3O_4 phase is the majority product of such a reaction, with CoOOH as a secondary product. It is shown that the Co_3O_4 phase results from the reaction of the CoOOH phase, formed by electrochemical oxidation of $Co(OH)_2$, with Co^{2+} species in the electrolyte, which is made possible by temperature. This process requires a global migration of the cobalt phases towards the current collector.

Keywords: Cobalt oxide; Alkaline batteries; Electro-oxidation

1. Introduction

Cobalt addition plays a key role to improve the performances of the nickel hydroxide electrode, the positive electrode of Ni-MH cell. Cobalt is usually added in two different ways to β-nickel hydroxide, the active material that stores energy: it can either be co-precipitated with nickel hydroxide, to form a mixed nickel–cobalt hydroxide, or post-added by mixing cobalt monoxide or cobalt hydroxide to nickel hydroxide. In co-precipitation, adding cobalt improves the conductivity of the active material [1,2] and reduces charge and discharge potential, compared to pure nickel hydroxide [3,4]. The conductivity increase as well as the decrease of the oxidation potential of the active material in charge, leads to an increased chargeability of the electrode and thus a higher capacity of the battery. Co-precipitation of cobalt in β-nickel hydroxide also tends to prevent the formation of the γ-type hydrated nickel oxyhydroxide phase during overcharge, and therefore the associated swelling of the electrode [5]. The life duration of the electrode is thus improved. In the case of post-added cobalt, the positive effect is linked to the high porosity of the nickel foam, used for non-sintered high-capacity electrodes, which plays both roles of substrate and current collector. Nickel hydroxide is filling the pores of the substrate. However, the low conductivity of the active material leads to isolating parts, which are located in the middle of the pores, and thus far away from the current collector. The result is a low active material utilization rate. When cobalt is added, either in the form of $Co(OH)_2$ or CoO, a conductive sub-network is formed within the pores, linking electronically the whole active material to the current collector, and thus allowing an active material utilization rate as high as 100% [6,7]. Such a role requires three main properties of the cobalt derivative: it is able to spread over the electrode, to form a wide conductive sub-network from localized addition; it forms a conductive phase after oxidation; the so-formed phase is stable in usual cycling conditions.

Though most of the work has been focused on the global performance of nickel hydroxide electrode, some studies have dealt with the mechanism of post-added cobalt effects. It has been shown that, whatever the cobalt phase added, it is oxidized into conductive CoOOH during the first charge [6]. Actually,

* Corresponding author. Tel.: +33 5 4000 2725; fax: +33 5 4000 6698.
E-mail address: guerlou@icmcb-bordeaux.cnrs.fr (L. Guerlou-Demourgues).

0378-7753/$ – see front matter © 2008 Elsevier B.V. All rights reserved.
doi:10.1016/j.jpowsour.2008.01.005

further work has demonstrated that the conductive phase was a non-stoichiometric H_xCoO_2 phase [8]. In the following the stoichiometric phase $HCoO_2$, which is a bad conductor, will be denoted as CoOOH. Two mechanisms were reported for the oxidation of $Co(OH)_2$ into CoOOH, depending on the charge rate [9]. At high charging rate, the oxidation proceeds via a solid-state reaction and the formed phase is the conductive H_xCoO_2 phase. At low charging rate, the CoOOH phase can also be formed by a dissolution–reprecipitation process. When CoO is used as an additive, it is hydrolyzed into $Co(OH)_2$. This step, occurring through dissolution–reprecipitation via the electrolyte, allows to better distribute the cobalt within the electrode and thus obtain a better effect of cobalt than with $Co(OH)_2$, for the same amount of cobalt added [6]. However, post-adding cobalt to the electrode exhibits some drawbacks. During storage at low potential, for example when a discharge cell is left in short circuit, cobalt is reduced and migrates to the surface of the current collector [10]. Such a phenomenon was already observed for co-precipitated cobalt [11]. The formation, in peculiar cycling conditions, of insulating phases like CoOOH [12,13] or Co_3O_4 [10,14], was also underlined, the latter phase being favored by higher temperature. Those studies pointed out the role of dissolved cobalt, as a blue cobalt complex formed in highly concentrated alkaline medium. These species were sometimes described as $HCoO_2^-$ [11,15]. More recent studies, based on visible spectroscopy, identified $Co(OH)_4^{2-}$ complexes [10,16] and a nucleation-growth mechanism in solution was proposed for the formation of Co_3O_4. A solution has been proposed to overcome the capacity loss by processing the first charge of the electrode, when the cobalt conductive network is formed, at 90 °C, which allows to maintain the performances of the electrode after a discharge or a storage at low potential [17]. These conditions tend to favor the formation of a Co_3O_4-type phase. Though the ideal Co_3O_4 phase is known as insulating, we could obtain Co_3O_4-type conductive phases (10^{-1} S cm^{-1}) by electro-oxidation of cobalt at 90 °C in different electrolytes [18]. The conductive phases were shown to be spinel-type cobalt derivatives, with the formula "$H_xLi_yCo_{3-z}O_4$", exhibiting cobalt vacancies, lithium, hydrogen and tetravalent cobalt in their structure. Such conductive phases were formed in LiOH electrolytes, but also in the ternary electrolyte (KOH, LiOH, NaOH) used in commercial cells, which is mainly constituted by KOH (approximately 8 M). Hence, to consider a less complicated chemical system though not too far from the commercial cells, the electrochemical oxidation of cobalt was studied in 8 M KOH. It was thus shown that in optimized conditions (CoO as starting phase and *C*/100 charge rate) a pure Co_3O_4-type phase was formed, with low conductivity but a structure close to the conductive phases. It is thus possible to investigate the formation mechanism of these phases in 8 M KOH.

In the present work, the behavior of cobalt derivatives during the charge at 90 °C in KOH 8 M is investigated. We focus on the mechanism leading to the Co_3O_4-type phase by studying the structural and morphological evolution of two different cobalt-starting phases: CoO and $Co(OH)_2$. The solubility of cobalt derivatives within the electrolyte and its evolution during electrochemical oxidation is also studied, to link the presence of $Co(OH)_4^{2-}$ species in the electrolyte to the formation of either Co_3O_4 or CoOOH. Finally, various KOH concentrations and charge rates were tested in order to confirm the proposed mechanism.

2. Experimental

All the materials were obtained by electro-oxidation of a cobalt-based electrode. The electrodes are made from a viscous paste consisting of CoO or $Co(OH)_2$, mixed with distilled water, that was introduced into porous nickel foam, dried 2 h at 85 °C and pressed at 1 t cm^{-2}. No mechanical binder such as PTFE was used, considering that only one charge is performed and that the material has to be recovered from the electrodes afterwards. The electrode was then set between two over-capacitive cadmium electrodes, playing both roles of counter electrode and reference electrode, with a polyamide separator avoiding short circuit. The electrolyte was 8 M KOH, but for additional experiments other concentrations between 1 M and 15 M were used. In the so-constituted Co–Cd cells, the cobalt-based electrode was the positive pole and the cadmium-based one the negative electrode. This convention will be used in the whole work, so that cell "charge" corresponds to cobalt oxidation. In the case of CoO as starting electrode material, the cells were kept 4 days at room temperature, after introducing electrolyte, to complete CoO hydrolysis into $Co(OH)_2$ before oxidation. They were then heated at 90 °C and charged at a *C*/100 rate, except for final experiments where various rates were used. Electrochemical oxidations were performed in a galvanostatic mode, with a homemade cycling apparatus and software. The recorded potentials are given vs. $Cd(OH)_2$/Cd electrochemical couple. Charge rates are given as *C*/*n*, meaning that one electron is exchanged per nickel or cobalt atom in *n* hours. After charge, electrodes were left 24 h in distilled water, with periodic change of the rinsing solution, in order to remove all trace of electrolyte. They were then dried one night at 60 °C and milled to complete an efficient recovery of the cobalt material. Separation of nickel, coming from the nickel foam, was performed by sieving on a sieve with 80 μm holes.

The X-ray diffraction (XRD) patterns were collected using either an INEL CPS 120 curve position sensitive detector with a cobalt anode or a Siemens D5000 diffractometer (Cu Kα). In the first case 1-h long acquisitions were performed; in the latter case, the data were recorded with a scan step of 0.02° (2θ) for 10 s.

Scanning electron microscopy (SEM) was performed upon pieces of electrode (approx. 2 mm × 2 mm) with a field effect gun Hitachi S4500 microscope. A 2-nm layer of platinum was previously sputtered on the samples to evacuate charges.

Cobalt in alkaline solution was titrated either by EDTA titration or by atomic absorption spectrometry at 242.5 nm using a PerkinElmer 2280 apparatus. Atomic absorption was preferred in the case of electrolyte testing during oxidation because the volume of available solution was low. In order to investigate the nature of cobalt in the electrolyte, UV–vis spectra were collected on a Varian Cary 5E apparatus in the 300–1200 nm wavelength range.

3. Oxidation of CoO- and $Co(OH)_2$-based electrodes at 90 °C in 8 M KOH

3.1. Electrochemical process and final materials

Electrodes containing CoO or $Co(OH)_2$ were electrochemically oxidized at a *C*/100 rate during 120 h at 90 °C in an 8 M KOH electrolyte. The electrodes containing CoO were previously hydrolyzed in the same electrolyte. A low charge rate (*C*/100) was chosen in order to avoid kinetic effects and to form the most stable phase in such temperature conditions.

The variations of cell potential vs. time, recorded for each synthesis cell, are presented in Fig. 1. The XRD patterns of the materials, recovered at the end of the charge, are displayed in Fig. 2. A pattern of the material recovered when processing the same experiment from CoO at room temperature (Fig. 2c) is displayed for comparison.

When the oxidation is performed at 90 °C from CoO as a starting material, the XRD pattern (Fig. 2a) shows the formation of a pure Co_3O_4-type phase, that has been more extensively described in a previous article [18]. It was shown that this phase exhibits some cobalt vacancies, contains structural hydrogen and presents an average cobalt oxidation state of 2.68. As shown in Fig. 1, the oxidation occurs on a plateau around 0.7 V vs. $Cd(OH)_2$/Cd, where 0.66 electrons are transferred per cobalt atom. This latter value is completely consistent with the oxidation of cobalt, initially at the oxidation state of 2 in the CoO starting material, to an oxidation state of 2.66, which is the average value in Co_3O_4. After this plateau, the potential increases, passes through a maximum and stabilizes around 0.95 V. This latter step is infinite and then should correspond to oxygen-evolution reaction, occurring when water in the electrolyte is oxidized into O_2. The increasing oscillations of potential could correspond to the formation of oxygen bubbles.

When $Co(OH)_2$ is used as starting material, as shown by XRD in Fig. 2b, a significant amount of the CoOOH phase is present in the sample together with the Co_3O_4 phase. The general shape of the oxidation curve looks like that observed from CoO (Fig. 1). The oxidation plateau takes place at a higher potential (0.8 V) and approximately 0.8 electrons are exchanged per cobalt atom on this plateau, which is consistent with the presence of the CoOOH phase, where cobalt is in a higher oxidation state than in Co_3O_4 (3 instead of 2.66). The potential maximum at the end of oxidation reaches a higher value than from CoO but the potential relaxes after too and the oxygen-evolution reaction takes place at a potential only 0.1 V higher than from CoO.

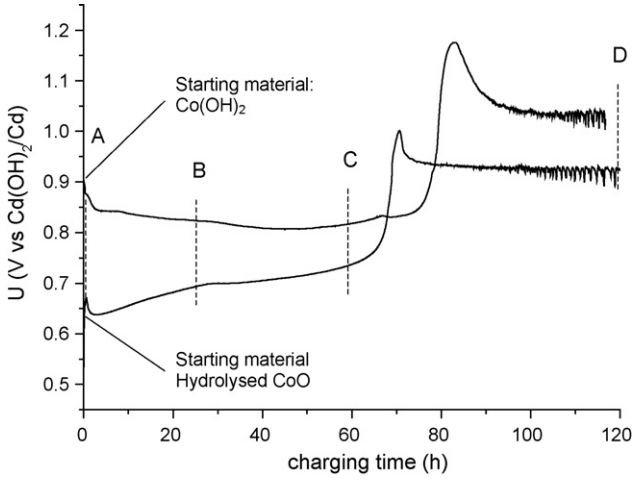

Fig. 1. Evolution of the potential vs. charging time during the first charge, at 90 °C, in 8 M KOH, with a *C*/100 charging rate, for an electrode initially pasted with CoO and hydrolyzed before charge and an electrode pasted with $Co(OH)_2$.

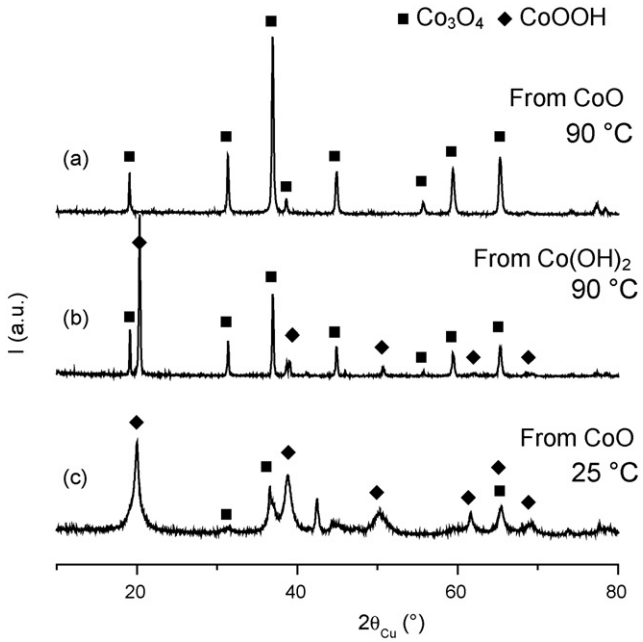

Fig. 2. XRD patterns of the materials obtained after 120 h of charge, in 8 M KOH, with a *C*/100 charging rate: (a) at 90° C from previously hydrolyzed CoO, (b) at 90 °C from $Co(OH)_2$ and (c) at 25 °C from previously hydrolyzed CoO.

At room temperature, as shown in Fig. 2c, a majority CoOOH phase is formed. This result is in accordance with various works that have shown that the CoOOH phase is formed at a potential of 0.9 V [13,19]. Moreover, some additional diffraction lines can also be seen, showing that a small amount of Co_3O_4 can be already formed at room temperature.

3.2. Structural evolutions of the materials during the oxidation

In order to understand how the Co_3O_4 phase is formed, various electrodes containing CoO were hydrolyzed for 4 days in 8 M KOH and then charged, at 90 °C, for various times, at the *C*/100 rate in the same electrolyte. Similar electrodes were prepared with $Co(OH)_2$ and directly charged in the same conditions. The materials were recovered just after hydrolysis (when necessary) and after 25, 60 and 120 h. These times are labeled as A, B, C and D, respectively on the charge curves of Fig. 1. The XRD patterns of the corresponding materials are displayed in Fig. 3 from CoO and in Fig. 4 from $Co(OH)_2$. The materials recovered after 120 h correspond to the final materials presented in the previous section (Fig. 2).

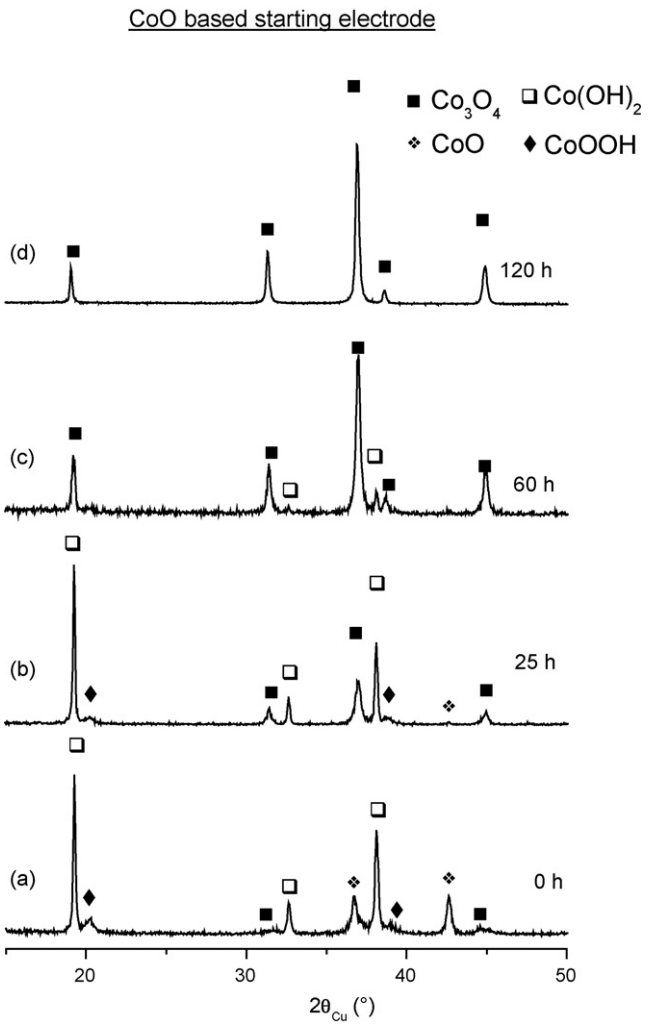

Fig. 3. XRD patterns of the materials obtained after a charge in 8 M KOH, with a *C*/100 charging rate, at 90° C, from previously hydrolyzed CoO: (a) starting material, (b) after 25 h of charge, (c) after 60 h of charge and (d) after 120 h of charge (same pattern as Fig. 2a).

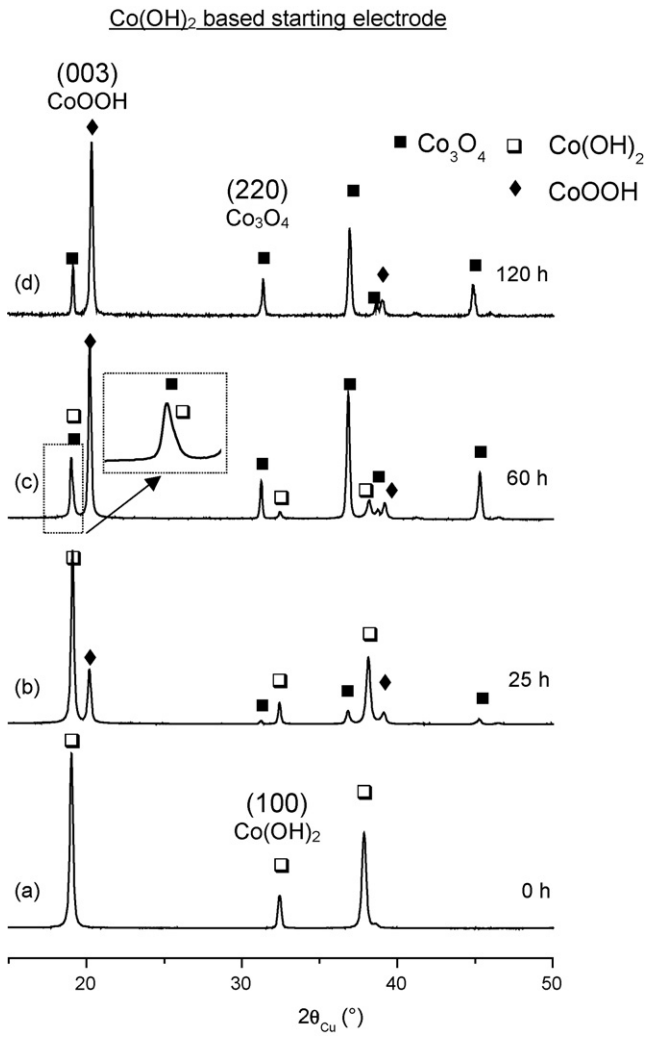

Fig. 4. XRD patterns of the materials obtained after a charge in 8 M KOH, with a *C*/100 charging rate, at 90 °C, from $Co(OH)_2$: (a) starting material, (b) after 25 h of charge, (c) after 60 h of charg and (d) after 120 h of charge (same pattern as Fig. 2b).

As shown in Fig. 3a, hydrolysis of CoO leads to a mixture that contains a majority $Co(OH)_2$ phase, remaining CoO and small amount of oxidized phases (CoOOH and Co_3O_4). These latter phases probably result from the oxidation of cobalt by dissolved oxygen. The XRD patterns of the other recovered electrodes (Fig. 3b and c) show a progressive decrease of the amount of $Co(OH)_2$ and a regular increase of the amount of Co_3O_4. The CoOOH phase disappears during the process.

In the case of the $Co(OH)_2$-based starting electrode, the amount of the CoOOH phase increases since the beginning of the charge. Most of the Co_3O_4 phase that is present in the final material seems to be formed from $Co(OH)_2$ only after 25 h of charge. At the end of the charge, the CoOOH phase has not disappeared.

These observations show that the main reaction is the transformation of $Co(OH)_2$ into Co_3O_4. But the question whether the formation of CoOOH is an intermediate stage or a concurrent reaction is raised. The earlier formation of CoOOH and the fact that this phase disappears when starting from CoO, is thus consistent with this phase being an intermediate. But the large amount of CoOOH at the end of the reaction, when starting from $Co(OH)_2$, is not consistent with such an hypothesis. This behavior will be explained in the final discussion.

To be more precise, in the case of the reaction from $Co(OH)_2$ (Fig. 4), where the three phases: $Co(OH)_2$, CoOOH and Co_3O_4 are simultaneously present in the electrodes, the approximate amounts of these cobalt phases were estimated on the basis of the XRD patterns. For this purpose, intensity ratios were taken as indicators, based on three non-overlapping diffraction lines of the three phases: (0 0 3) line for CoOOH at 20.3° ($2\theta_{Cu}$) (2 2 0) line for Co_3O_4 at 31.5° and (1 0 0) line for $Co(OH)_2$ at 32.4°. From a general viewpoint, in a binary mixture of two phases (A and B) and considering one diffraction line of the XRD pattern for each phase (respectively line A and line B), the weight fraction of phase A is expected to be equal to the ratio: (area line A)/[(area line A) + k(area line B)], where k is a factor depending on the relative intensity of the considered lines, and the natures of both phases. Several binary mixtures in various

Table 1
Composition of the recovered material after different charging times during the charge of a $Co(OH)_2$-pasted electrode

	Oxidation time			
	0 h	25 h	60 h	120 h
$Co(OH)_2$ wt.%	100	63	12	0
CoOOH wt.%	0	30	38	39
Co_3O_4 wt.%	0	7	50	61

These values were evaluated by comparing the surface of the peaks on the patterns of Fig. 4.

proportions of CoOOH and Co_3O_4 powders and of $Co(OH)_2$ and Co_3O_4 powders were thus prepared and investigated by XRD. In the case of the CoOOH/Co_3O_4 mixtures, the k factor was empirically determined in order to minimize the difference between the $(0\,0\,3)_{CoOOH}/[k(2\,2\,0)_{Co_3O_4} + (0\,0\,3)_{CoOOH}]$ ratio and the weight fraction of CoOOH in the various samples. The same procedure was used for $Co(OH)_2/Co_3O_4$ mixtures. Hence the resulting ratio $(0\,0\,3)_{CoOOH}/[8(2\,2\,0)_{Co_3O_4} + (0\,0\,3)_{CoOOH}]$ was taken to evaluate the CoOOH weight fraction (vs. Co_3O_4) in the electrochemically synthesized samples and the $(1\,0\,0)_{Co(OH)_2}/[1.25(2\,2\,0)_{Co_3O_4} + (1\,0\,0)_{Co(OH)_2}]$ ratio was taken for the $Co(OH)_2$ weight fraction (also vs. Co_3O_4). Both weight fractions lead to the composition of the samples. The difference between the ratios deduced from XRD with the prepared weight fraction was less than 10% for the calibration mixtures. The calculated proportions are reported in Table 1. Even though these proportions do not give the exact values of the weight percentages, the accuracy is good enough to highlight some tendencies. The main deviation should indeed especially come from the phases used for the standard mixtures that exhibit probably crystallites sizes different from the phases in the electrodes. The values in Table 1 confirm that the CoOOH phase is formed in a first step and Co_3O_4 in a second step, and that the CoOOH formed does not disappear during the second step. Logically the amount of $Co(OH)_2$ decreases progressively during the charge.

4. Behavior of $Co(OH)_2$ and CoOOH at 90 °C in 8 M KOH

Three additive experiments have been carried out to investigate different mechanisms that are likely to be involved in the formation of Co_3O_4.

First, an electrode, containing CoO, was hydrolyzed for 4 days in 8 M KOH at room temperature and then maintained 120 h at 90 °C. This treatment at 90 °C induces very small changes (results not shown) in comparison to electrodes hydrolyzed at room temperature (Fig. 3a) and composed of a majority $Co(OH)_2$ phase, remaining CoO and small amount of CoOOH and Co_3O_4. Only the traces of the CoOOH phase disappear. This shows that the transformations during the electrochemical oxidation cannot be due to temperature only.

Second, an electrode, containing ex situ prepared CoOOH, was also charged at the same rate and temperature in 8 M KOH. This CoOOH phase was obtained by simultaneous precipitation of $Co(OH)_2$ and oxidation by adding a $Co(NO_3)_2$ solution to NaClO/KOH mixture. Except for a noticeable recrystallization of the phase, no significant change was observed after electrochemical oxidation at 90 °C (results also not shown here). The direct evolution of CoOOH could thus not lead to Co_3O_4. It should, however, be noticed that during this experiment, the potential was maintained at 1.2 V by charging, which could possibly hinder the reduction of CoOOH.

Third, 750 mg of a mixture of CoOOH and $Co(OH)_2$ in 2/1 molar proportions, previously ground in a mortar, were let in 20 mL of 8 M KOH, at 90 °C, during 15 h. The experi-

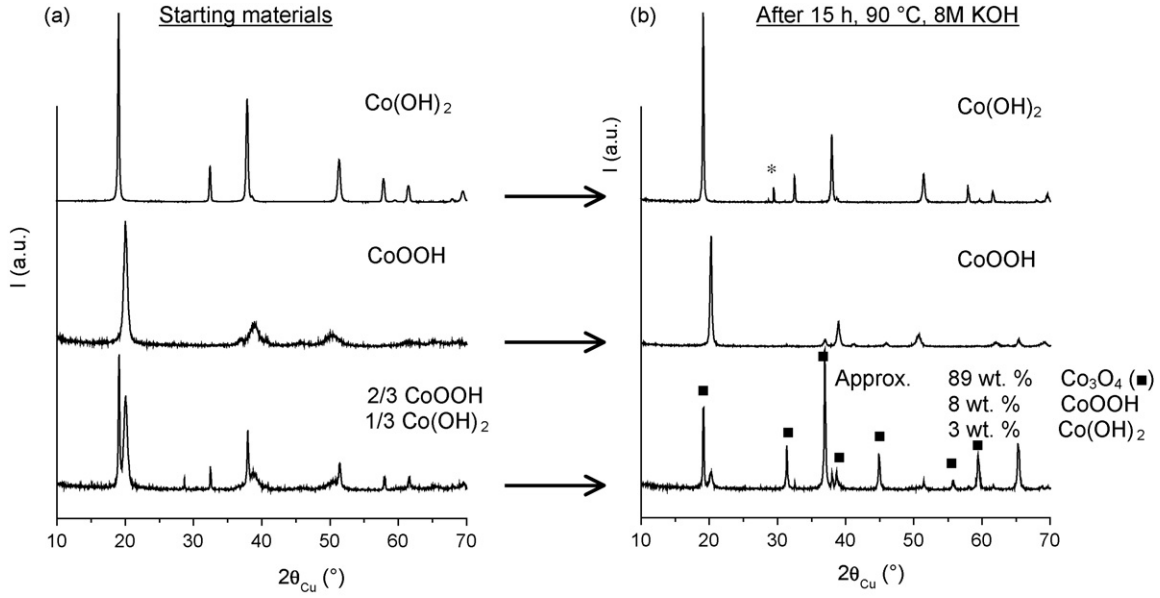

Fig. 5. XRD patterns of the materials submitted to treatment at 90 °C, in 8 M KOH, during 15 h. (a) Starting materials: $Co(OH)_2$, CoOOH, mixture (1/3)$Co(OH)_2$ (2/3)CoOOH. (b) After treatment (* potassium salts from electrolyte).

ment was performed in an air-tight container without stirring. The $Co(OH)_2$ phase was the same as for electrochemical experiments and the CoOOH phase had been obtained by the same way as for the previous experiment. Similar experiments were processed with the starting materials separately. XRD patterns of the starting materials (a) and the final materials (b) are presented in Fig. 5. With the single phases ($Co(OH)_2$ or CoOOH) as starting phases, the patterns of the final materials indicate very few changes, except for a noticeable recrystallization shown by the narrower diffraction lines, especially in the case of CoOOH. On the contrary, when starting with the CoOOH/$Co(OH)_2$ mixture, a nearly complete chemical reaction takes place, leading to Co_3O_4 (Fig. 5b). The proportions of the phases, indicated in Fig. 5b, have been calculated using the diffraction lines area ratio method already used in the previous section. The CoOOH phase, resulting from the oxidation of $Co(OH)_2$, can thus disappear to form the Co_3O_4 phase, following the reaction: $Co(OH)_2 + 2CoOOH \rightarrow Co_3O_4 + H_2O$. This reaction is necessarily taking place during the electrochemical oxidation, since the CoOOH and $Co(OH)_2$ are present together during the electrochemical oxidation at 90 °C in 8 M KOH (see previous section).

4.1. Textural aspects

A SEM study of the electrodes before and after charge shows a major evolution of the aspect of the electrodes in the case of both starting materials: hydrolyzed CoO (Fig. 6a and b) or $Co(OH)_2$ (Fig. 6c and d). Both electrodes before charge have a similar aspect: cobalt material fills the porosity of the nickel foam. After 120 h of oxidation, both types of electrodes exhibit a porous aspect and the whole material is located around the nickel foam, forming a shell. These views account for a global migration of the cobalt phases from the inside of the pores to the surface of nickel foam during the charge. Such a long-range transport suggests a mechanism via the solution.

We could also observe the cross-section of the shell surrounding the nickel foam after the charge of hydrolyzed CoO and $Co(OH)_2$ as starting materials, in some places where the oxide coat was broken. The views are presented in Fig. 7. The shell is composed of two layers (Fig. 7a1 and a2) with CoO as starting material and three layers (Fig. 7b1–b3) in the case of $Co(OH)_2$. In both cases, the external layers are very thin (Fig. 7a1 and b1). It should also be remembered that the XRD patterns of both corresponding materials, already presented in Fig. 3d and 4d, have shown that the material obtained from CoO consists of the

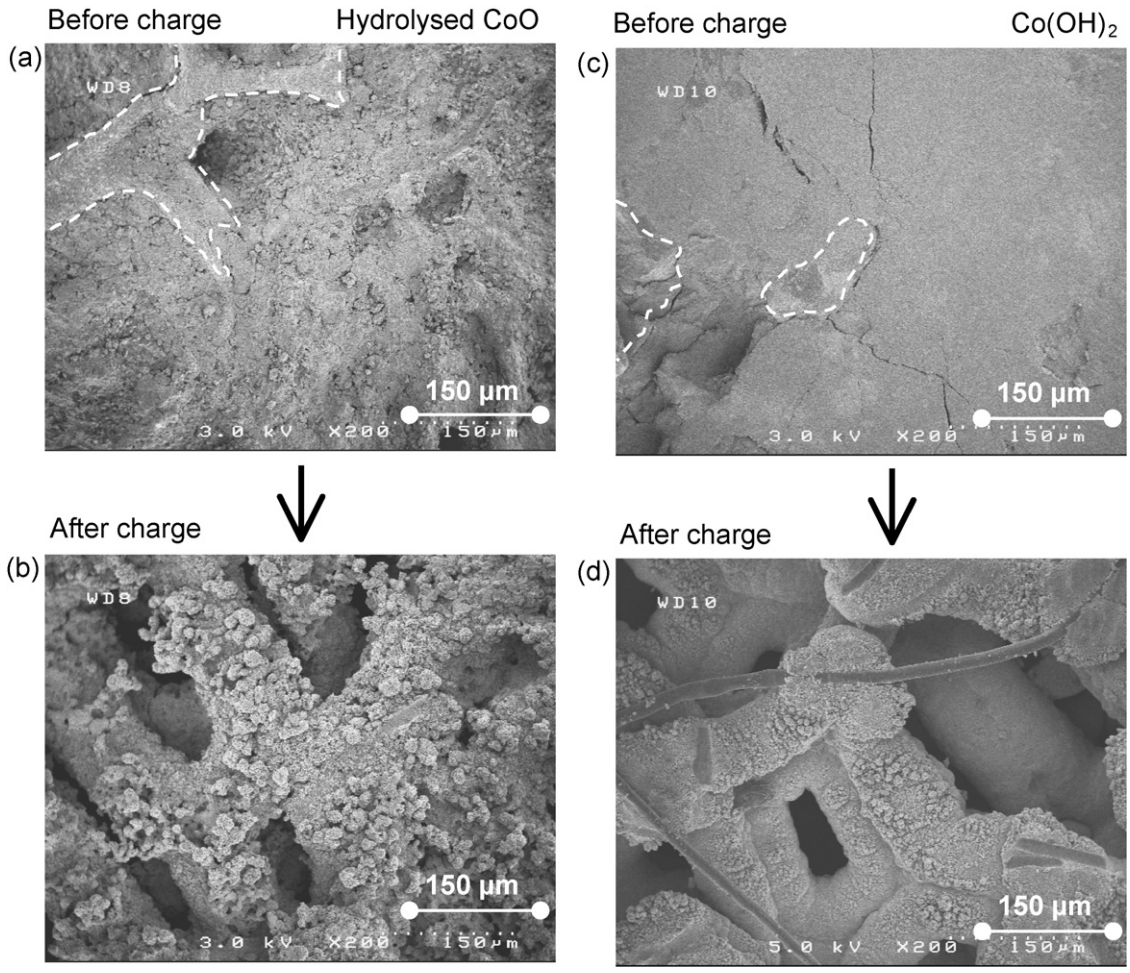

Fig. 6. SEM pictures (200×) of electrodes pasted with CoO and $Co(OH)_2$: (a) electrode pasted with CoO after hydrolysis, (b) the same after 120 h charge at 90 °C, (c) electrode pasted with $Co(OH)_2$ and (d) the same after 120 h charge at 90 °C. Dashed white lines correspond to the outline of the nickel foam.

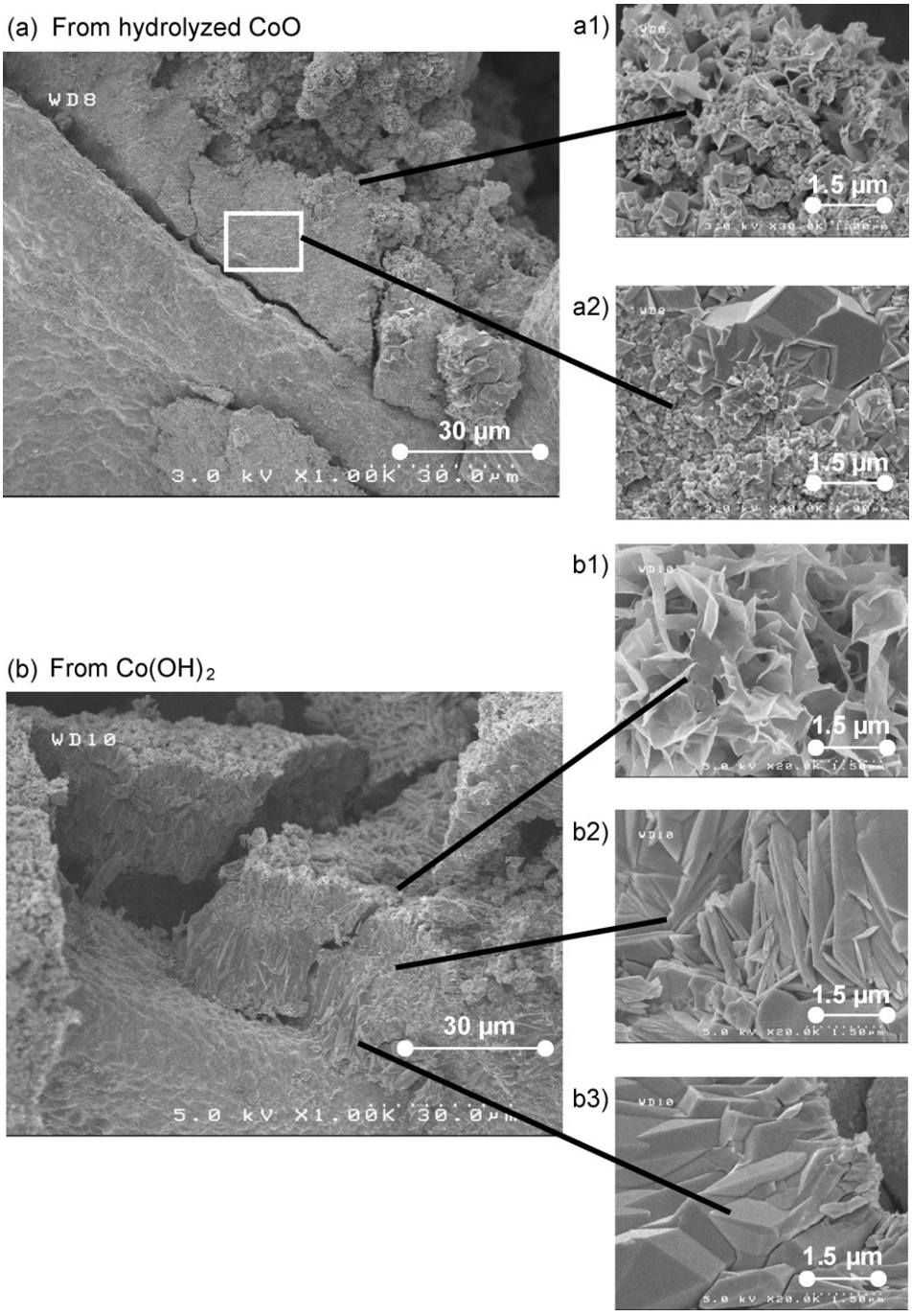

Fig. 7. SEM pictures of the cross-section of the shell made of cobalt oxide and hydroxide, surrounding the nickel foam, after a charge at 90 °C in 8 M KOH: (a) general view (1000×) for a starting CoO-pasted electrode, (a1) zoom (30,000×) of the texture at the surface of the shell, (a2) zoom (×30,000) of the bulk of the shell, (b) general view (×1000) for a starting $Co(OH)_2$-pasted electrode, (b1) zoom (20,000×) of the texture at the surface of the shell and (b2) and (b3) zoom (20,000×) on two different layers forming the bulk of the shell.

Co_3O_4 phase, while that obtained from $Co(OH)_2$ is a mixture of Co_3O_4 and CoOOH in similar proportions.

When the starting material is CoO (Fig. 7a), the material within the thick layer (Fig. 7a2), consists of a compact packing of irregular crystal. Considering the XRD pattern, this material is Co_3O_4.

When the starting material is $Co(OH)_2$ (Fig. 7b), two thick layers can be observed in the cross-section. The layer closer to the nickel foam (Fig. 7b3) is constituted of irregular crystals, the texture of which is very similar to that observed from CoO (Fig. 7a2). Therefore, we assigned this layer to Co_3O_4. The layer surrounding the previous one is formed by platelet-type particles (Fig. 7b2), which can be assigned to the CoOOH phase. The observed similar thickness of both layers, though difficult to evaluate, seem to be consistent with the proportions of the two phases suggested by XRD pattern. These textural features with both starting materials are schematically summarized in Fig. 8.

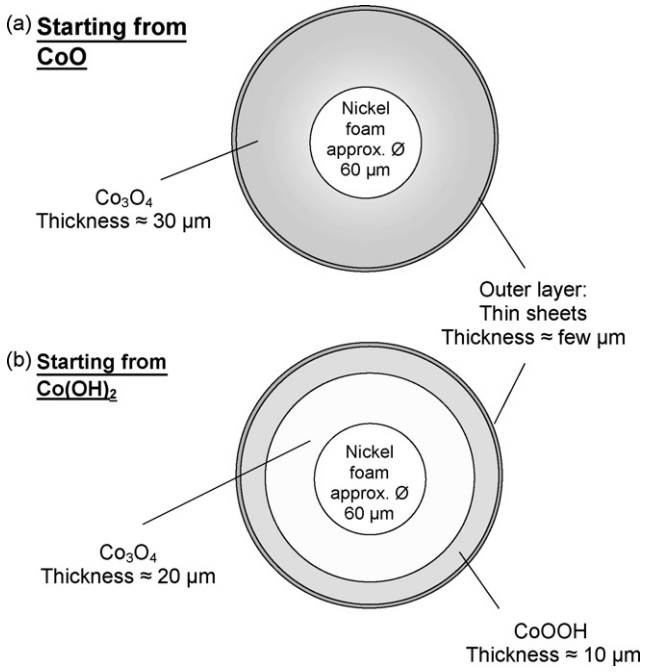

Fig. 8. Schematic representation of the repartition of the cobalt phases deposited at the surface of the nickel foam after a charge, at 90 °C, in 8 M KOH, for (a) a previously hydrolyzed CoO pasted electrode and (b) a $Co(OH)_2$ pasted electrode.

Other SEM observations (not presented here) have shown that in both cases, the superficial layer, made of thin foils (Fig 7a1–b1), is formed just after the potential maximum has been reached on the charge curve (Fig. 1). Such texture could thus be linked to the oxygen-evolution reaction.

As a conclusion, two main points should be extracted from the SEM study. First, the material migrates at relatively long range during the process, suggesting a mechanism involving dissolution and transport trough electrolyte. Second, the Co_3O_4 phase seems to be formed in both studied cases around the current collector.

4.2. Cobalt in the electrolyte

The cobalt species dissolved within the electrolyte were investigated in order to confirm the mechanism of transport via the solution. Such mechanism was suggested by textural features and by the structural changes, required to transform the lamellar $Co(OH)_2$ phase into cubic Co_3O_4.

Whatever the charging time, the electrolyte has a blue color, which is consistent with the color reported for cobalt complexes in basic solution [10,15]. UV–vis spectroscopy experiments were performed upon these electrolytes. The recorded spectrum for the electrolyte recovered during charge of a previously hydrolyzed CoO electrode is presented in Fig. 9. The spectrum collected for 50 mL of an 8 M KOH solution, held 15 h at 90 °C with 2 g $Co(OH)_2$ therein, is displayed for comparison. The comparison of the spectra shows a similar position in the two cases for the three absorption peaks at 533, 584 and 629 nm. These absorptions are likely to correspond to Co^{2+} in tetrahedral environment [10], confirming that the blue cobalt complex involved is $Co(OH)_4^{2-}$.

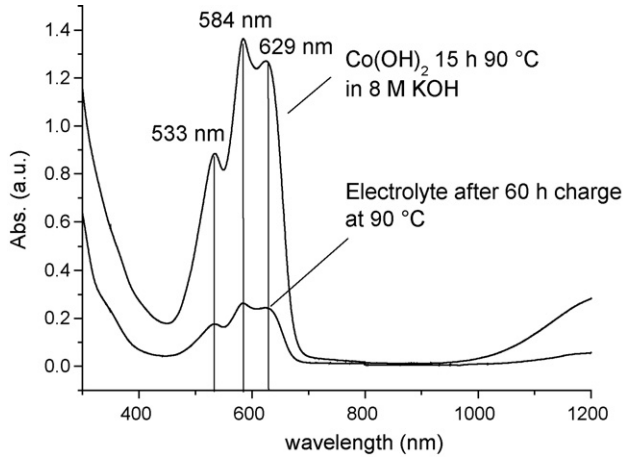

Fig. 9. UV–vis spectrum of the electrolyte recovered during the charge of a previously hydrolyzed CoO electrode. The spectrum of an 8 M KOH solution, in which $Co(OH)_2$ was dissolved at 90 °C, during 15 h, is displayed as reference.

Table 2
Cobalt concentration in different KOH solutions, after storage of 2 g of $Co(OH)_2$ in 50 mL of solution, at 90 °C, during 15 h

[KOH] (M)	[Co] (mg L^{-1})
1	20
5	130
8	375
15	1050

In addition, the solubility in KOH electrolytes of the different cobalt phases: $Co(OH)_2$, CoOOH, CoO, likely to be involved in the formation mechanism of Co_3O_4, were measured. For this purpose, 2 g of $Co(OH)_2$ or CoOOH or 1.6 g of CoO, these weights corresponding to similar cobalt amounts, were placed in an air-tight container with 50 mL of electrolytes with various concentrations (1, 5, 8 and 15 M), during 15 h, at 90 °C. The cobalt concentrations in the solutions were then measured by EDTA titration as described in the experimental part. The evolution of the solubility of $Co(OH)_2$ as a function of KOH concentration (1–15 M range) is presented in Table 2. The solubilities of the other studied phases in 8 M KOH can be compared in Table 3. The first point is that the solubility of $Co(OH)_2$ increases regularly with KOH concentration, as shown in Table 2. In 8 M KOH (Table 3), the resulting amount of cobalt in solution is higher, when the starting material is $Co(OH)_2$ rather than CoO. In the case of CoOOH, no significant amount of cobalt is detected in solution.

After these preliminary experiments, the evolution of the cobalt concentration in the electrolyte (8 M KOH) was followed

Table 3
Cobalt concentration in 8 M KOH solutions, after storage of 2 g of $Co(OH)_2$, CoOOH or 1.6 g of CoO in 50 mL of solution, at 90 °C, during 15 h

	[Co] (mg L^{-1})
$Co(OH)_2$ 90 °C	375
CoO 90 °C	135
CoOOH 90 °C	0

by atomic absorption spectroscopy, during the charge, at 90 °C, of CoO- and $Co(OH)_2$-based electrodes, at the *C*/100 charge rate. Among the 75 mL used as electrolyte for a test cell, 2–2.5 mL were taken out at several times; 1 mL was diluted between 50 and 200 times in distilled water and the cobalt concentration was measured. It should be noted that such way of proceeding, convenient because only a small amount of electrolyte was needed for each measurement, leads to a relatively high incertitude (approx. ±15%). The evolutions of the cobalt concentration in the electrolyte vs. time are presented in Fig. 10 for both experiments (starting with CoO or with $Co(OH)_2$). In both cases, cobalt concentration increases during the first 20 h of charge, then seems to decrease slightly until the end of reaction (corresponding to the increase in potential on the charge curve in Fig. 1), where the cobalt concentration drops to a value as small as 15 mg L^{-1} in both cases. The measured cobalt concentration is significantly higher in the case of a starting $Co(OH)_2$ phase, reaching a maximum value of 130 mg L^{-1}, while 80 mg L^{-1} is the maximum value when starting from CoO.

This behavior can be explained with the results reported in the previous sections. The increase in cobalt concentration in the electrolyte, during the 1st hours, is probably linked to the kinetics of dissolution of $Co(OH)_2$ at 90 °C. The limitation of the cobalt concentration after 25 h and the fact that the maximum values reached for CoO and $Co(OH)_2$ (respectively 80 and 130 mg L^{-1}) are much lower than the values of solubility reported in Table 3 (135 and 375 mg L^{-1}), suggest that cobalt in electrolyte is consumed by a reaction. This reaction could correspond to that shown in a previous section, for a 2:1 mixture of CoOOH and $Co(OH)_2$. In this case, this reaction is likely to process between the CoOOH phase in the solid state and Co^{2+} ions within the solution (actually $Co(OH)_4^{2-}$ complexes), coming from dissolution of $Co(OH)_2$. Such mechanism is in accordance with the cobalt concentration dropping from the electrolyte as soon as the $Co(OH)_2$ phase has disappeared.

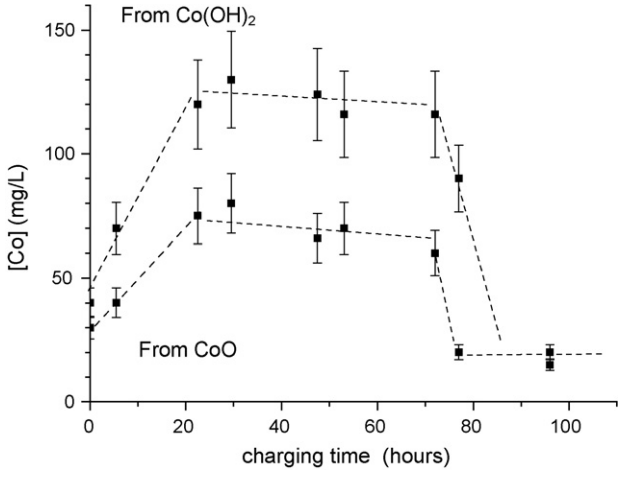

Fig. 10. Evolutions of the concentration of cobalt in the electrolyte vs. charging time, during charges, at 90 °C, in 8 M KOH, of a previously hydrolyzed CoO electrode and of a $Co(OH)_2$ electrode.

4.3. Influence of charging rate and electrolyte concentration

In the previous sections, the electrochemical oxidation of the cobalt phases has been studied in conditions (8 M KOH and *C*/100) which have been optimized to lead to a single Co_3O_4 phase with CoO as starting material. In these conditions, the formation of Co_3O_4 and CoOOH, starting from $Co(OH)_2$ (which is also formed from hydrolysis of CoO), occurs with two different kinetics. The material resulting from the electrochemical process should thus depend on the charge rate. Besides, part of the process involves a mechanism via the solution. As we previously showed that $Co(OH)_2$ solubility is related to KOH concentration, the final material should also depend on the electrolyte concentration.

Electrodes, prepared with CoO, were previously hydrolyzed and then charged (with 150% overcharge) at 90 °C, on the one hand in 8 M KOH at various charge rates and on the other hand in various KOH concentrations at *C*/100 charge rate. The weight fractions of CoOOH were evaluated in the materials recovered after the charge. For this purpose, the intensity ratio previously used in this paper was considered: $(0\,0\,3)_{CoOOH}/[8(2\,2\,0)_{Co_3O_4} + (0\,0\,3)_{CoOOH}]$, this ratio being a good approximation of the CoOOH weight fraction in a Co_3O_4/CoOOH binary mixture. The evolutions of the weight fraction of CoOOH in the recovered samples as a function of charge rate or KOH concentration are displayed in Fig. 11a and b, respectively.

As shown in Fig. 11a, the amount of the CoOOH phase in the recovered samples increases with increasing charge rate (in 8 M KOH), from 0% at the *C*/100 charge rate up to 12% at C/2. Such evolution suggests that formation of CoOOH is quicker than formation of Co_3O_4, which is consistent with the results of Table 1.

As shown in Fig. 11b, the amount of the CoOOH phase in the recovered samples increases with decreasing KOH concentration (with a *C*/100 charge rate). A lower cobalt concentration, obtained with a lower KOH concentration (see previous section), thus slows down the formation of Co_3O_4.

5. Discussion upon cobalt oxidation mechanism

We propose a global mechanism for the electrochemical oxidation of cobalt phases in 8 M KOH at 90 °C, based on the previous experiments The proposed mechanism should explain the differences between hydrolysed CoO and $Co(OH)_2$ as starting materials, the textural features, the values of cobalt concentration in the electrolyte during the charge, and the influence of the charge rate and KOH concentration.

With the cobalt derivatives, the following reactions are well known:

$$CoO + H_2O \rightarrow Co(OH)_2 \qquad \text{(hydrolysis of CoO)} \qquad (1)$$

$$Co(OH)_2 \rightarrow CoOOH + H^+ + e^-$$

$$\text{(electrochemical oxidation of } Co(OH)_2\text{[9, 19])} \qquad (2)$$

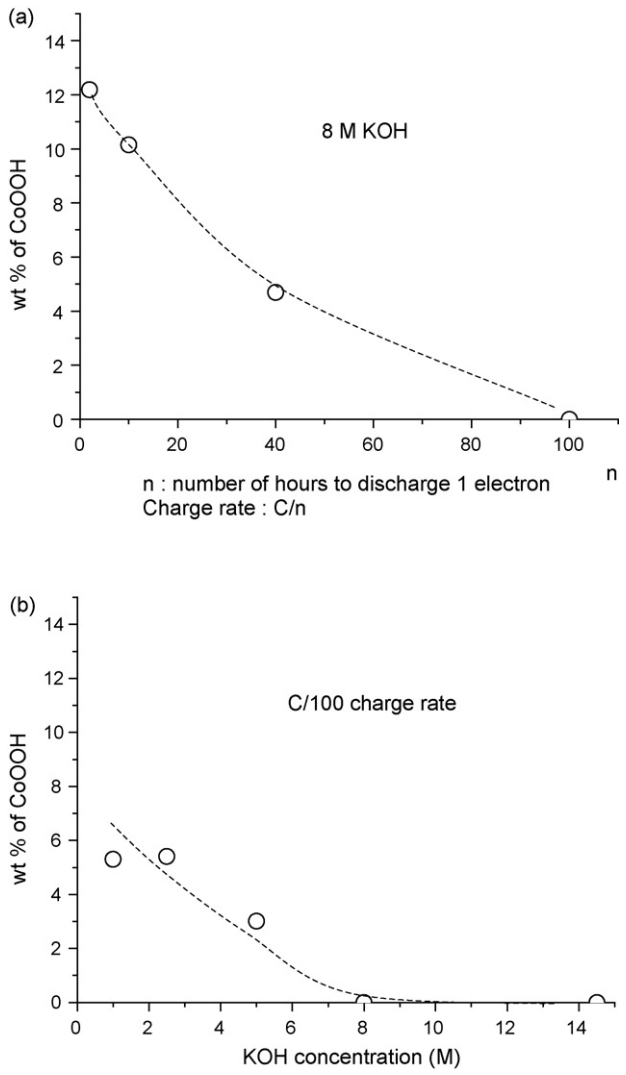

Fig. 11. Evolutions of the weight content of the CoOOH phase vs. (a) charge rate and (b) KOH concentration, in the material recovered after a charge, at 90 °C, of a previously hydrolyzed CoO electrode.

$$Co(OH)_2 + 2OH^- \rightarrow Co(OH)_4^{2-} \quad (\text{solubility of } Co(OH)_2) \tag{3}$$

The feasibility of the following reaction has also been demonstrated in this paper:

$$Co(OH)_2 + 2CoOOH \rightarrow Co_3O_4 + 2H_2O \tag{4}$$

But since that reaction is not likely to occur in the solid state at 90 °C, the real reaction is probably

$$Co(OH)_4^{2-} + 2CoOOH \rightarrow Co_3O_4 + 2H_2O + 2OH^- \tag{5}$$

Hence, as the starting electrode (after hydrolysis from CoO) contains $Co(OH)_2$, the reactional pathway is probably a classical electrochemical oxidation of $Co(OH)_2$ into CoOOH (2) followed by a reaction of CoOOH with Co complexes in the electrolyte in solution (5). The role of the temperature is to increase the solubility of cobalt and also the kinetics of reaction (5). The initial temperature of the formation of the electrode (90 °C) is therefore a key point for the cycling performance, because the solubility of cobalt and the kinetics of reaction (5) influence the amounts of Co_3O_4 (which brings the high level of electronic conductivity) and of remaining CoOOH (which entails a bad behavior in the case of a deep discharge). In other terms, a temperature lower than 90 °C will tend to decrease the amount of Co_3O_4 in favor of CoOOH, and the electrochemical performance will be poorer.

The hydrolysis of CoO (1) is likely to lead to much smaller particles of $Co(OH)_2$ than those of a commercial product used as starting phase. Because of the low charge rate, the kinetics of reaction (2) should not be significantly affected. But bigger particles of $Co(OH)_2$ will lead to bigger particles of CoOOH, which should react much more slowly with cobalt complex in solution, resulting in a much slower formation of Co_3O_4. As schematized in Fig. 12, this could account for the compositions and the textures of the electrodes: the CoOOH phase begins to form close to the current collector, then the earlier formed CoOOH will be transformed into Co_3O_4 and the CoOOH is continuously formed further away from the current collector. The reaction stops when there is no remaining $Co(OH)_2$. If the formation of Co_3O_4 (reaction (5)) is fast, all the CoOOH is

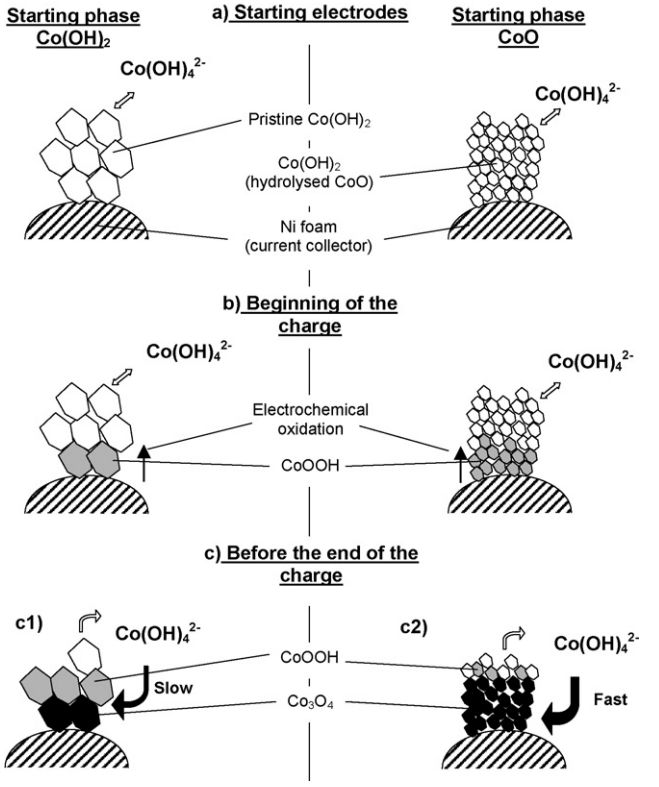

Fig. 12. Schematic representation of the processes involved during the charge at 90 °C of an electrode containing hydrolysed CoO or $Co(OH)_2$: (a) electrodes before charge illustrating morphologic differences between pristine $Co(OH)_2$ and $Co(OH)_2$ resulting from CoO hydrolysis; (b) beginning of charge: oxidation of $Co(OH)_2$ into CoOOH; (c) before the end of the charge: CoOOH and $Co(OH)_4^{2-}$ react together to form Co_3O_4: (c1) the reaction is slow. Later formed CoOOH will remain in an external layer, (c2) the reaction is fast. All CoOOH will be transformed in Co_3O_4.

transformed. If reaction (5) is slow, CoOOH is remaining in the external layer (formed later).

This mechanism could also account for the differences in the cobalt concentration in the electrolyte. Reaction (5) is consuming cobalt in the electrolyte, which is continuously produced by dissolution of $Co(OH)_2$ (3). If reaction (5) is fast, the concentration of cobalt in the electrolyte would thus be lower than if it is slow.

Finally, the influence of KOH concentration and charge rate upon the nature of the final material is also completely consistent with such mechanism. A higher charge rate should favor the formation of CoOOH, as observed (Fig. 11a). A higher KOH concentration favors cobalt dissolution (Table 2); the cobalt concentration would then be higher and thus the formation of Co_3O_4 faster, resulting in the presence of less CoOOH in the final material (Fig. 11b).

6. Conclusion

We have shown that, in 8 M KOH, performing the electro-oxidation of cobalt at a low charging rate, at 90 °C rather than at room temperature, favors the formation of a Co_3O_4-type phase at the expense of the CoOOH phase, usually formed at room temperature. The formation of this phase is favorised by a low charge rate and a high KOH concentration. With optimized conditions, *C*/100 charge rate and at least 8 M KOH concentration, a single Co_3O_4-type phase can be formed.

Having pure Co_3O_4, without CoOOH, as conductive additive in the electrode is very interesting, because the structure of this Co_3O_4 phase was shown through voltammetry studies to be stable at very low potential, down to −0.4 V vs. Hg/HgO [12,17], contrarily to CoOOH, which is reduced into $Co(OH)_2$ at −0.2 V, and dissolved in the electrolyte [10]. Consequently, the results reported in this paper suggest to perform an initial electro-oxidation at 90 °C of CoO, rather than $Co(OH)_2$, to obtain a ratio Co_3O_4/CoOOH as high as possible and a maximal stability of the conductive network at low potential (deep discharge or long-term floating).

As far the mechanism of cobalt oxidation and formation of Co_3O_4 is concerned, high temperature for an aqueous medium has been shown to increase $Co(OH)_2$ solubility and thus to allow the reaction between the CoOOH phase, formed by electrochemical oxidation, and the cobalt in solution ($Co(OH)_4^{2-}$ complexes).

Moreover, this study shows again, how complex the mechanisms involving cobalt are, in alkaline batteries. For example in an electrode initially containing only CoO, four different cobalt phases are present after hydrolysis: CoO, $Co(OH)_2$, Co_3O_4 and CoOOH (Fig. 3a). In the present conditions, most of these studied phases are metastable. The properties of the various materials can also significantly depend on the texture, as shown by the totally different electrochemical behavior obtained starting from $Co(OH)_2$, either prepared ex situ or obtained by hydrolyzing CoO.

Acknowledgements

The authors thank C. Mathoniere for UV–vis measurements, M. Basterreix and C. Denage for technical assistance, Saft, ANRT and Région Aquitaine for financial support.

References

[1] Y. Borthomieu, Thesis of University Bordeaux I, (1990).
[2] A. Cressent, V. Pralong, A. Audemer, J.B. Leriche, A. Delahaye Vidal, J.M. Tarascon, Solid State Sci. 3 (2001) 65.
[3] P. Oliva, J. Leonardi, J.F. Laurent, C. Delmas, J.J. Braconnier, M. Figlarz, F. Fievet, A. De Guibert, J. Power Sources 8 (1982) 229.
[4] L. Guerlou-Demourgues, C. Delmas, J. Electrochem. Soc. 141 (1994) 713.
[5] M. Oshitani, T. Takayama, K. Takashima, S. Tsuji, J. Appl. Electrochem. 16 (1986) 403.
[6] M. Oshitani, H. Yufu, K. Takashima, S. Tsuji, Y. Matsumaru, J. Electrochem. Soc. 136 (6) (1989) 1590.
[7] M. Oshitani, M. Watada, T. Tanaka, T. Iida, Electrochem. Soc. Proc. Ser. 94–27 (1994) 303.
[8] M. Butel, L. Gautier, C. Delmas, Solid State Ionics 122 (1999) 271.
[9] V. Pralong, A. Delahaye-Vidal, B. Beaudoin, B. Gérand, J.M. Tarascon, J. Mater. Chem. 9 (1999) 955.
[10] V. Pralong, A. Delahaye Vidal, B. Beaudoin, J.B. Leriche, J. Scoyer, J.M. Tarascon, J. Electrochem. Soc. 147 (6) (2000) 2096.
[11] A.H. Zimmerman, R. Seaver, J. Electrochem. Soc. 137 (9) (1990) 2662.
[12] M. Butel, Thesis of University Bordeaux I, (1998).
[13] V. Pralong, A. Delahaye-Vidal, B. Beaudoin, J.B. Leriche, J.M. Tarascon, J. Electrochem. Soc. 147 (4) (2000) 1306.
[14] S. Aravamuthan, C.V. Annamma, M.J. Nair, J. Power Sources 50 (1994) 81.
[15] M. Pourbaix, Atlas d'équilibres électrochimiques, Gauthier Villars Paris, 1963, p. 342.
[16] B. Ezhov, O.G. Malandin, Extended Abstracts of the 40th ISE Meeting, Kyoto, Japan, 1989, p. 454.
[17] K. Yuasa, Japanese Patent, JP 2003-031216 (2003).
[18] F. Tronel, L. Guerlou-Demourgues, M. Ménétrier, L. Croguennec, L. Goubault, P. Bernard, C. Delmas, Chem. Mater. 18 (25) (2006) 5840.
[19] P. Benson, G.W.D. Briggs, W.F.K. Wynne-Jones, Electrochim. Acta (1964) 281.